PLASMA PROCESSING R&D FOR THE SNS SUPERCONDUCTING LINAC RF CAVITIES*

M. Doleans, R. Afanador, J. Ball, W. Blokland, M. Crofford, B. Degraff, D. Douglas, B. Hannah,
M. Howell, S-H. Kim, S-W. Lee, C. McMahan, J. Saunders, P. V. Tyagi,
ORNL, Oak Ridge, TN 37831, USA

Abstract

The Spallation Neutron Source routinely operates with a proton beam power of 1 MW on its production target. A plan to reach the design 1.4 MW within a few years is in place [1] and relies on increasing the ion beam current, pulse length and beam energy in the linac. The increase in beam energy from the present 930 MeV to 1 GeV will require an increase of approximately 15% in the accelerating gradient of the superconducting linac high-beta cryomodules. In-situ plasma processing was identified as a promising technique to reduce electron activity in the SNS superconducting cavities and increase their accelerating gradient [2]. R&D on plasma processing aims at deploying the new in-situ technique in the linac tunnel by 2016. Overall plan and current status of the plasma processing R&D will be presented.

INTRODUCTION

Medium-beta (MB) superconducting cavities at the SNS operate above design gradients while high-beta (HB) cavities operate bel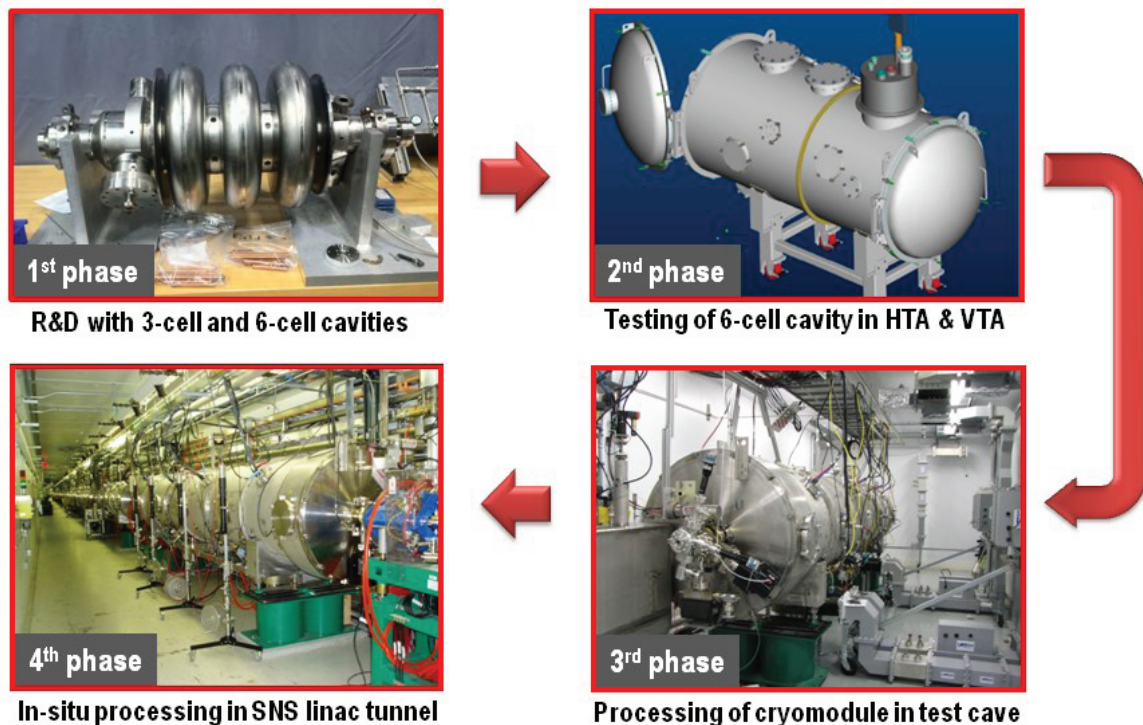ow design gradients, mainly due to electron activities and in particular due to field emission. The electrons emitted from the surface are accelerated by the RF electric field before striking and heating the Niobium surface of the resonators leading to thermal instabilities, mostly in the cavity end-groups.

As explained in [2], the accelerating gradients that can be run stably in the superconducting linac (SCL) at the SNS strongly depends on the repetition rate. The higher the repetition rate, the lower the accelerating gradients before reaching thermal instability in the cryomodules. At 10 Hz repetition rate, and with cavities powered individually, the average stable accelerating gradient for the HB section is about 30% higher than at the nominal 60 Hz repetition rate with all the cavities powered simultaneously. A 15% increase of the accelerating gradients of the SCL HB cryomodules is being pursued using in-situ plasma processing. A similar idea is being considered at JLAB to benefit CEBAF operation [3].

Figure 1: Strategy for the development of plasma processing technique at the SNS.

Previous studies [2] and RGA measurement during thermal cycling of cryomodules have shown that residual contamination, for example from hydrocarbons, is a source of field emission in the SNS SCL resonators.

In-situ plasma processing aims at removing residual surface contamination, particularly hydrocarbons from the HB cavity inner surfaces. No plasma etching technique like in [4] is being pursued at this point in time at the SNS. Also, no electron cyclotron resonance is used to excite the plasma as in [5] because it wouldn't be suitable for in-situ plasma processing of the SNS cryomodules.

A microwave discharge in an SRF cavity can be generated at room temperature or at cryogenic temperature. Because cold surfaces can cryo-pump the volatiles compounds desorbed from the surface, plasma processing at room temperature is preferred.

Because deploying a new technique in an operating superconducting linac presents inherent risks, a progressive strategy in four phases has been devised and is shown in Figure 1:

- Plasma processing studies with 3-cell and 6-cell cavities
- Cold-test of plasma processed cavities
- Plasma processing of an offline cryomodule
- Deployment of in-situ plasma processing in the SNS linac tunnel

The plasma processing of an offline cryomodule will be facilitated by the fact that the SNS has recently built a spare HB cryomodule [6].

Figure 2: Plasma processing in a 6-cell beta=0.81 cavity at the SNS.

PLASMA PROCESSING AT THE SNS

The first phase of the plasma processing R&D is on-going. Preparatory work for the second phase has started and cold-test of plasma processed cavities are planned in FY14 using the new vertical test area (VTA) and horizontal test apparatus (HTA) [7,8]. The VTA and HTA use the new Cryogenic Test Facility (CTF) [9].

Plasma Processing Station

A plasma processing station was developed during the first phase of the R&D. This station is mounted on a movable rack and is shown in Figure 2. In its present configuration it has two RF generators, a 500 W solid

state amplifier, a circulator and a load capable of supporting full reflection, and a crate for control of the RF and recording of all the instruments. The amplifier has a center frequency of 805 MHz and a +-25 MHz tuning range.

Instrumentation connected to the crate includes vacuum gauges, RF generator and power meters, video cameras, RGA, optical spectrometer and thermocouples. Most of the data acquisition has been done through Labview and post-processing is done using DIAdem. DIAdem is an ideal data visualization tool for this type of R&D because it easily handles heterogeneous types of data, it has a high level script language and can be used to replay plasma processing studies with synchronization of all the instrument signals. An example of such a sequence is illustrated in Figure 3.
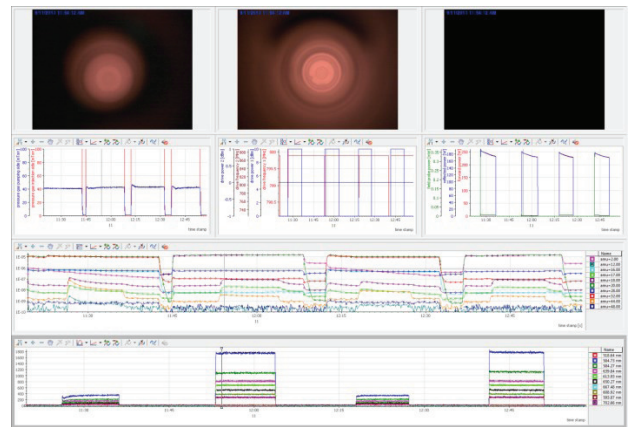

Figure 3: Example of a plasma processing sequence post-processed and visualized in DIAdem.

Plasma Ignition

To ignite a plasma in the cavity, a flow of neutral gas is created through the cavity volume and one of the fundamental passband mode is excited until a microwave discharge occurs. The mode frequency and field amplitude in each cell of a multicell cavity is given by [10]

$$\Omega_m = \frac{\omega_m^2}{\omega_0^2} = 1 + k\left[1 - \cos\left(\frac{m\pi}{N}\right)\right]$$

$$|m\rangle_j = \sqrt{(2 - \delta_{mN})/N} \, \sin\left((j - 1/2)\frac{m\pi}{N}\right) \quad (1)$$

Where the zero index refers to the frequency of a single-cell cavity, the m index refers to the mth mode, and the index j runs from 1 to N, N being the number of cells.

The fundamental mode resonant frequencies and on-axis field profiles for the 3-cell MB cavity and several 6-cell HB cavities used in the R&D have been measured and closely follow Equation 1. As expected, all cavities had a few percents deviation of their field intensities with respect to the ideal model.

09 Cavity preparation and production
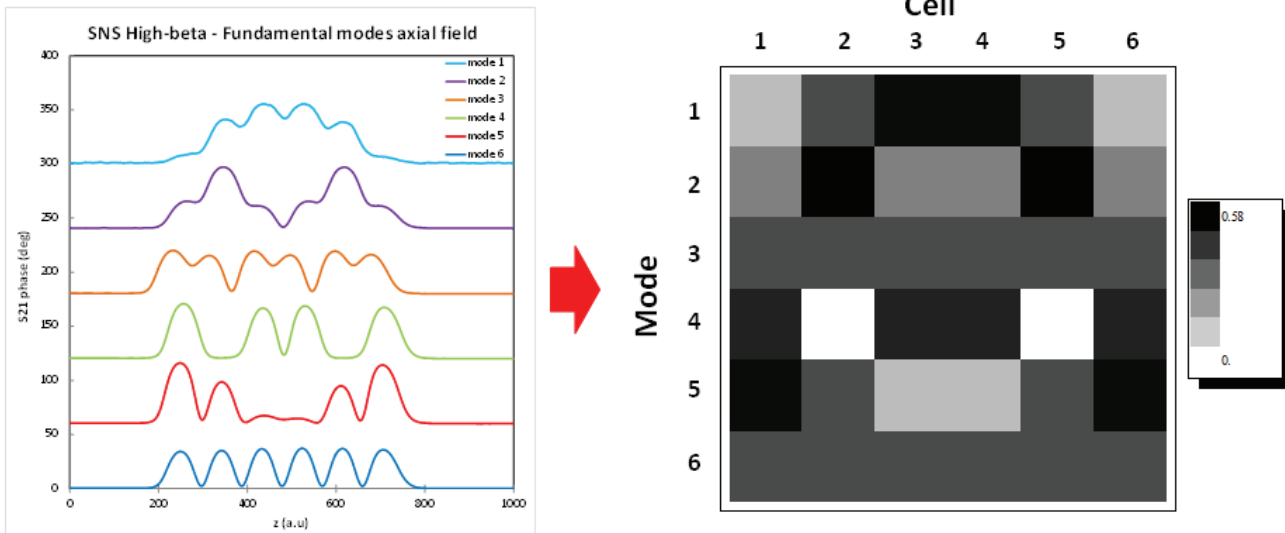
H. Basic R&D bulk Nb - Other processing

Figure 4: (left) on-axis field measurement for the six fundamental passband modes a SNS HB 6-cell cavity. (right) matrix plot of the ideal normalized field amplitudes .

As an example, the on-axis field profile measurement for the six fundamental modes in a 6-cell HB cavity is shown in Figure 4. A convenient 6x6 matrix plot also shows the field amplitude for all modes and in each cell of the resonator.

The plasma ignition condition in a cavity depends on the gas specie and pressure and has similar features to the Paschen curve for a DC discharge [11]. Ignition curves for the 3-cell medium beta cavity are shown in Figure 5. Ignition was achieved in the cavity volume for various gases and for the three modes of the 3-cell cavity. Plasma ignition in the fundamental power coupler instead of in the cavity volume can also occur but an acceptable range of gas pressure and forward power could always be found to ignite a plasma in the cavity.
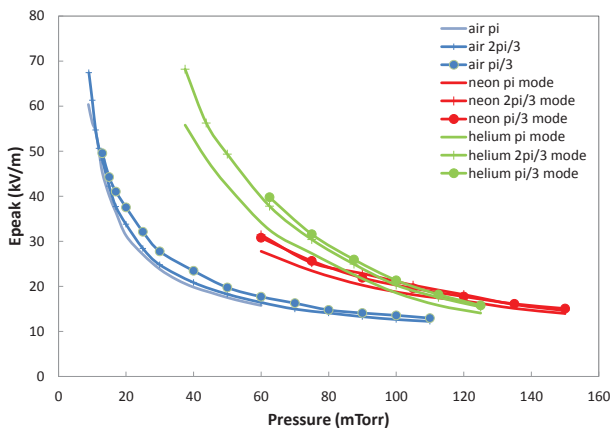
Because the amplitude of the electric field in each cell depends on which mode is being excited, the plasma can be ignited at various locations in the resonator. As an example, a helium plasma ignited in the 6th cell or in the 2nd cell of a HB cavity is shown in Figure 6.

Plasma Tuning

The plasma ignited in a cavity acts as a dielectric [12] with dielectric constant less than unity. The plasma dielectric constant depends on the plasma density and is given by

$$\varepsilon = 1 - \eta$$

$$\eta = \frac{\omega_{plasma}^2}{\omega_{rf}^2} \qquad . \qquad (2)$$

$$f_{plasma} \propto \sqrt{n_{plasma}}$$

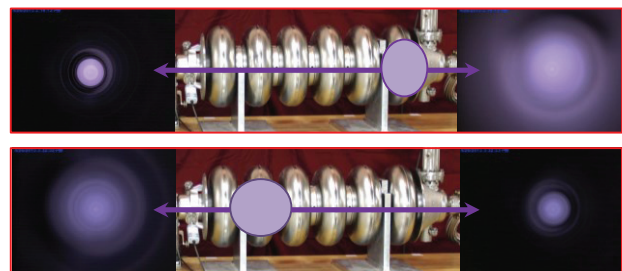Figure 5: Plasma ignition in a 3-cell MB cavity as a function of the gas pressure and peak surface electric field.

Figure 6: Helium plasma in a 6-cell HB cavity in the 6th cell (top row) and 2nd cell (bottom row). Depending on its location, the plasma appears closer or farther away from the axial cameras used at each end of the resonator.
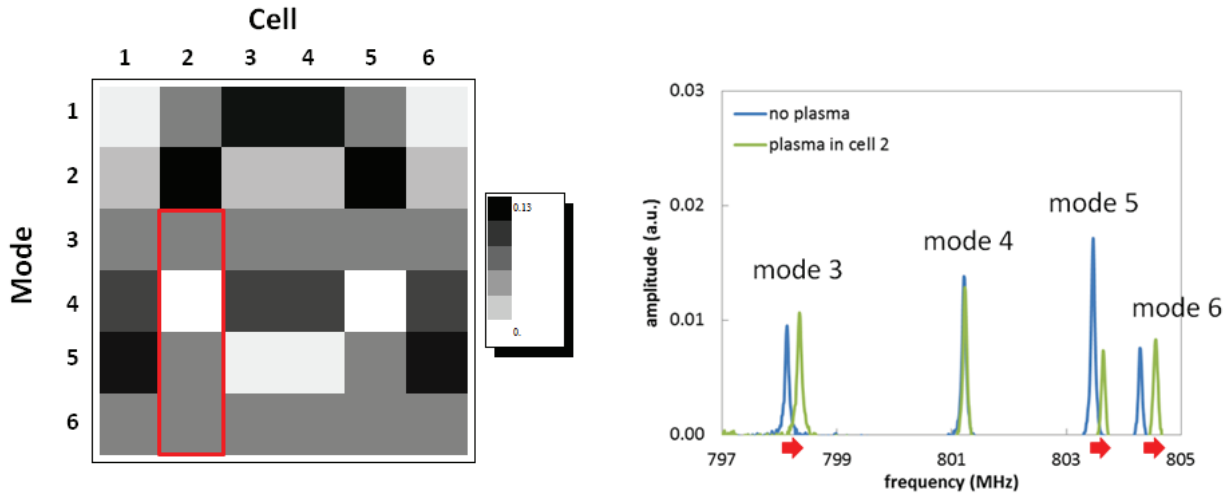
Figure 7: (left, model) Perturbation of the resonance frequency (a.u) due to a plasma in each of the six cells of the cavity and for each of the six fundamental passband modes of a HB cavity. (right, experiment) Measurement of the resonance modes for modes 3 to 6 without (blue) and with (green) plasma ignited in the 2nd cell of the cavity. Only modes 3, 5 and 6 are shifted, while mode 4 frequency remains unchanged, as expected from the model (see red contour in the left plot)

When a resonant structure is loaded by a plasma, its resonant frequency is shifted upward [13]

$$\frac{\delta\omega}{\omega} = \frac{1}{2(1+\beta^2)} \frac{\iiint_{plasma} \eta E^2 dV}{\iiint_{cavity} E^2 dV} \qquad (3)$$

$$\beta = \frac{\upsilon_{e-neutral}}{\omega_{rf}}$$

At our working pressure the collisional effect of the electron on the neutral gas can be neglected (i.e. $\beta \ll 1$). The mode characteristics (i.e. resonant frequencies and field patterns) depend in which cells the plasma has ignited. When the plasma loading effect is treated as a perturbation, the description of the mode characteristics closely resembles the one used for field flatness tuning of a multicell cavity [10]. For example if one writes the perturbation matrix due to the plasma as

$$P = \begin{pmatrix} \eta_1 & 0 & 0 \\ 0 & \ddots & 0 \\ 0 & 0 & \eta_N \end{pmatrix} \qquad (4)$$

one can write the perturbation effect on the resonant frequencies and field amplitudes as

$$\Omega'_m = \Omega_m + \langle m|P|m \rangle$$

$$|m\rangle' = |m\rangle + \sum_{n \neq m} \frac{\langle n|P|m \rangle}{\Omega_m - \Omega_n} |n\rangle \qquad (5)$$

To illustrate this effect, a matrix plot showing the shift in the mode resonant frequencies caused by a plasma in each of the cells of a cavity is shown in Figure 7. To check the basic validity of this model, a plasma was ignited in the 2nd cell of a 6-cell HB cavity by using the 2nd mode. Resonances of mode 3 to 6 were monitored simultaneously through the field-probe signal. As expected from the model, the resonance frequency for modes 3, 5 and 6 are all shifted upward while the one for mode 4 is left unchanged. This is because the 4th mode has no stored energy in the 2nd cell.

As shown in Equation 5, the relative field amplitude in the cells of a resonator is also affected by the ignition of a plasma. Figure 8 shows the perturbation on the amplitude of the electric field, for all modes and in each cell, due to the ignition of a plasma at different locations in the cavity.

The modelling of the perturbation from a plasma in the resonator provides relevant information to tune the plasma. To increase the plasma density, the RF generator frequency should be raised as to track the upward shift of the mode resonances. It should be noted that when this is done, the increase in the plasma density then leads to a larger shift in the resonance frequency and the processes can be iterated to further increase the plasma density. To ignite the plasma in multiple cells, the variation of the field amplitude as illustrated in Figure 8 can be utilized.
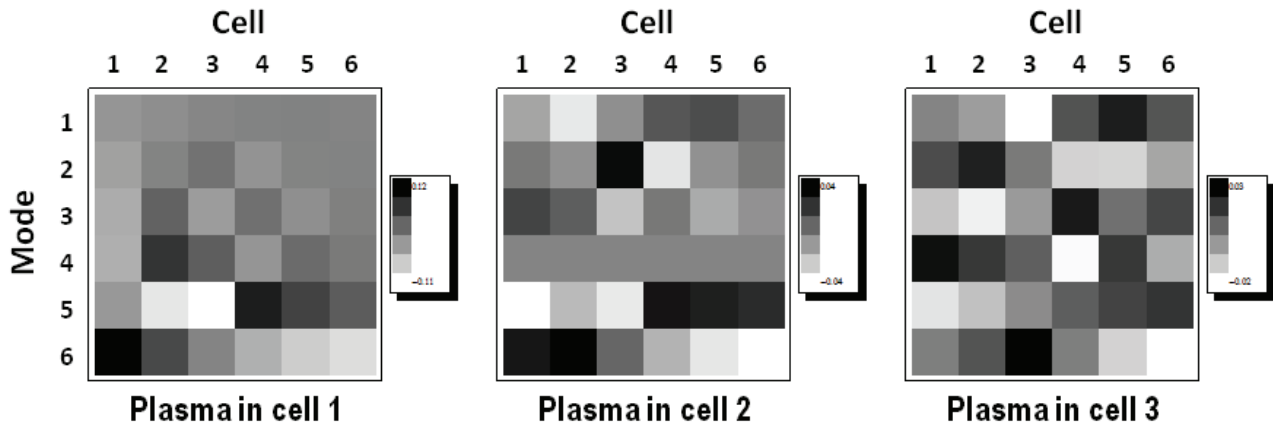
Figure 8: Perturbation of the field amplitude for all fundamental passband modes and in each cell of 6-cell cavity due to the presence of a plasma at various location in the resonator. Results for a plasma ignited in cell 1, 2 or 3 are presented. Results for cells 4, 5 and 6 can found by mirror symmetry.

For example, one sees that the 5th mode is adequate to ignite a plasma in the two end cells of the resonator. For this mode, when the plasma ignites in one end cell, the field amplitude increases in the opposite end cell of the cavity such that the ignition level in that cell can be reached. Similarly, the 1st mode is adequate to ignite a plasma in the two center-cells.

Plasma Chemistry and Cleaning

Plasma chemistry is a vast and rich topic [14]. The mechanisms of the plasma-chemical processes can be quite complex because the plasma is inherently a highly reactive system with multi-components chemically active. All the charged particles, excited atoms and molecules, radicals and UV photons can play an active role and lead to physical, chemical and photochemical processes.

In our case, the physical energy of the ions is too small to initiate significant physical action and the plasma processes are dominated by chemical and photochemical effects. It is thus very improbable to find one plasma processing method to get rid of all possible residual contaminants on the operating SNS cavities.

We have purposefully decided to focus primarily on the removal of hydrocarbon residues from the surface because it is believed that their cleaning could lead to significant mitigation of the field emission affecting the SNS HB cavities. But, even in this case, the task of cleaning hydrocarbons from a niobium surface is far from trivial since cleaning and redepositing processes happen simultaneously. When a chemically active plasma is generated it is as critical to monitor the possible creation of new chemical bonds on the surface as it is to monitor the cleaning of the surface contaminants.

Niobium samples introduced in the cavity volume provide a convenient method to learn and study plasma chemistry for SRF cavities. Because we decided to study the removal of hydrocarbons, FTIR technique [15] was used to analyse the hydrocarbons on the niobium surface of the samples. FTIR, and particularly specular reflectance method [16] was used because it is a fast analysis technique that doesn't require UHV or sample preparation, it is non-destructive so that the same samples can be analysed before and after plasma processing, and it provides chemical bond information about the surface contaminants. Of course, FTIR also has its limitations and the use of complementary surface analysis techniques is being pursued.

Plasma processing of hydrocarbon was attempted using a Ne-O_2-H_2 mixture. Neon was used as a support gas because it was found to create very stable discharges during plasma tuning studies. Oxygen is used as a cleaning agent because it can oxidize the surface carbon to CO and CO_2, which easily desorb. And it can also react with the surface hydrogen and desorb in water and hydroxyl form [17-19]. However, it can also attach during the process [20]. For this reason, hydrogen was added to the mixture. Surface carbon is hydrogenated to hydrocarbon molecules and oxygen can be removed by creating and desorbing water and hydroxyl molecules [21].

Four Niobium samples (flat disks of 25mm diameter and 1 mm thickness) were contaminated using a black permanent marker which contains long hydrocarbon chains such as n-propanol and n-butanol [22]. The samples were introduced in the 3-cell MB cavity. Two were positioned close in the iris region of the end cells, and the other two far away from any electric field in the end flanges region as shown in Figure 9. FTIR spectra for all samples before plasma processing are shown in Figure 10. The complexity of the hydrocarbon composition of the marker is evident from the broadness and multiplicity of the peaks in the FTIR spectra.
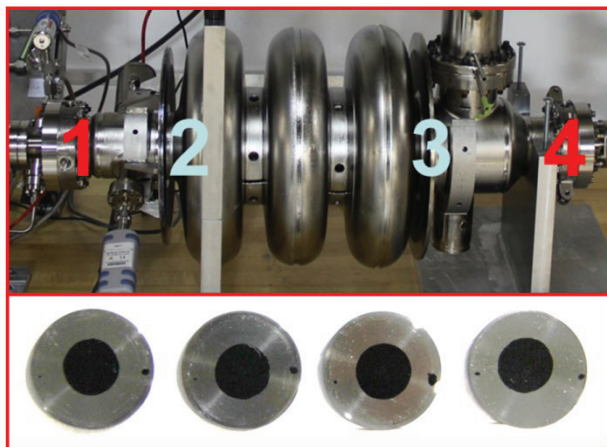
Figure 9: Four Nb samples before introduction into the 3-cell MB cavity. The samples were purposefully contaminated to study the cleaning of hydrocarbon chains by a plasma.

A plasma using a Ne-O_2-H_2 mixture was ignited using the second mode and tuned up such that a plasma was present in both end-cells of the cavity volume. As expected, increase in the RGA signals for masses 18, 28 and 44 were observed when the plasma was ignited corresponding to removal of hydrocarbons from the samples in the form of water, carbon monoxide and carbon dioxide. The plasma was left on for a few hours. The four samples were then removed from the cavity volume for inspection.
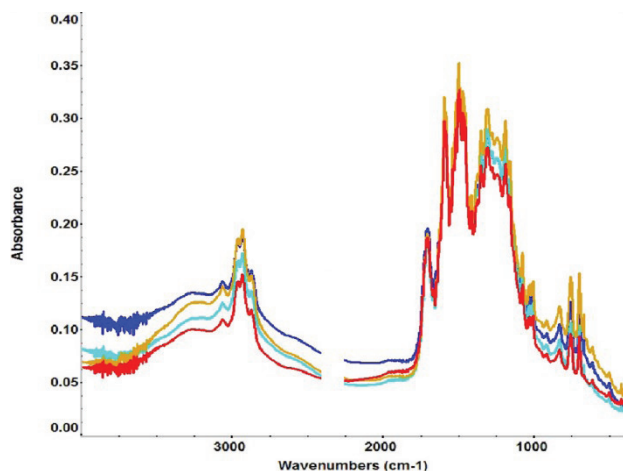

Figure 10: FTIR specular reflectance spectra for the four Niobium samples before plasma processing.

Images of the samples after plasma processing are shown in Figure 11, and the corresponding FTIR spectra are shown in Figure 12. The two samples positioned close to the plasma in the end-cells were significantly cleaned by the plasma, while the other two samples located in the end-flanges outside of the plasma do not appear significantly changed. Furthermore, the FTIR spectra reveal that all the types of hydrocarbon bonds were successfully processed and that no new chemical bonds were formed on the sample surface (i.e. no new peaks

were detected). But, complementary analysis techniques such as XPS or SIMS [15] should be performed on the processed samples to confirm this point. It is believed that the remaining traces of contamination on sample 2 and 3 could be removed using additional plasma processing.

Figure 11: Nb samples after plasma processing in Ne-O_2-H_2mixture. The samples positioned near the end cells of the cavity were cleaned while the samples located near the end flanges remain basically unchanged.
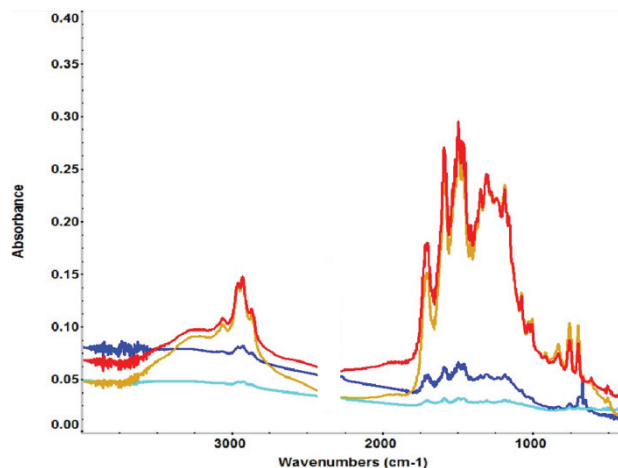

Figure 12: FTIR specular reflectance spectra pectra for the four Niobium samples after plasma processing.

CONCLUSION

Plasma processing R&D at the SNS is on-going and aims at providing an in-situ technique to remove residual contamination for the SC cavities operated in the linac. Results from the first phase of the R&D are promising and the second phase of the R&D will start in FY14 and include cold-test of plasma processed cavities.

ACKNOWLEDGMENT

REFERENCES

[1] Neutron Sciences Directorate Five year plan 2012-2016, August 2012, SNS-NSCD-EXE-PN-0001, R00, Oak Ridge National Laboratory.

[2] S-H Kim et al., "R&D Status for In-Situ Plasma Surface Cleaning of SRF Cavities at Spallation Neutron Source", Proceedings of 2011 Particle Accelerator Conference, New York, NY, USA.

[3] J. Mammosser et al., "Large-volume Resonant Microwave Discharge for Plasma Cleaning of a

CEBAF 5-cell SRF Cavity", Proceedings of IPAC2012, New Orleans, Louisiana, USA.

[4] M. Raskovic, "Plasma treatment of bulk niobium surface for superconducting rf cavities: Optimization of the experimental conditions on flat samples" PRSTAB **13**, 112001 (2010).

[5] G. Wu et al., "Plasma cleaning: towards high yield cavity processing", TFSRF 2008, JLAB.

[6] M. Howell et al., "The First ASME Code Stamped Cryomodule at SNS," IPAC'12, New Orleans, LA, May 2012, p. 2465 (2012).

[7] S.H. Kim et al., "The Status of Superconducting Linac and SRF Activities at the SNS", Proceedings of the 16th International Conference on RF Superconductivity, Paris, France, 2013.

[8] J. Saunders et al, "Status of SRF Facilities at SNS," IPAC'12, New Orleans, LA, May 2012, p. 2471 (2012).

[9] M. Howell et al, "Status of Spallation Neutron Source Cryogenic Test Facility (CTF)," submitted to PAC'13, Pasadena, CA, September 2013.

[10] H. Padamsee, J. Knobloch and T. Hays, "RF Superconductivity for Accelerators" Wiley series in beam physics and accelerator technology, ISBN 0-471-15432-6.

[11] S. C. Brown, "Introduction to Electrical Discharges in Gases" Wiley series in plasma physics.

[12] S. Bastian, Notes on electromagnetic waves in a plasma, National Radio Astronomy Obsevatory, Charlottesville, VA, 2005.

[13] S. C. Brown Microwave Studies of Gas Discharge Plasmas, P/387 USA.

[14] A. Fridman, "Plasma Chemistry" Cambridge University Press, ISBN-13 978-0-511-40243-2.

[15] J. Vickerman and I. Gilmore, "Surface Analysis - The Principal Techniques" J. Wiley & Sons, Ltd. DOI: 10.1002/9780470721582.

[16] .Setnicka, FT-IR Reflection Techniques.

[17] R. E. Kirby et al., Linear Collider Collaboration Tech Notes, LCC-0075, Novemberr 2001, Stanford Linear Accelerator Center, Stanford, CA.

[18] A. Belkind et al., "Oil removal from metals by linear multi-orifice hollow cathode", Surface and Coatings Technology 76-77 (1995) 738-743.

[19] H. Li et al., "An in situ XPS study of oxygen plasma cleaning of aluminum surfaces", Surface and Coatings Technology 92 (1997) I71-177.

[20] A. Vesel, "Modification of polystyrene with a highly reactive cold oxygen plasma", Surface & Coatings Technology 205 (2010) 490–497.

[21] P. Kruger, R. Knes and J. Friedrich, "Surface cleaning by plasma-enhanced desorption of contaminants (PEDC)", Surface and Coatings Technology 112 (1999) 240–244.

[22] C. Moody, Black writing ink analysis by direct infusion electrospray mass spectrometry, M.S. Thesis, University of central Florida, (2010).